Applied Mathematical Sciences, Vol. 1, 2007, no. 26, 1249 - 1263

The Flow Separation through Peristaltic Motion for Power-law Fluid in Uniform Tube

Abd El Hakeem Abd El Naby and M.F. Abd El Kareem

Department of Mathematics, Faculty of Science, Mansoura University,

P.O. 34415, New Damietta, Egypt

Abstract

The flow separation (trapping) at the wall through peristaltic motion for non-Newtonian power-law fluid in uniform tube has been investigated under zero Reynolds number with long wavelength approximation. A condition frequently used to predict separation in boundary layer theory is to set the vorticity equal to zero on the boundary. We solve the problem numerically to get flow separation points on the wall surface. It has been noted that, the trapping region decreases with increasing volume flow rate but it increases with increasing power-law index n. Furthermore, the shearing extra stress increases with increasing volume flow rate. Also, it increases with n at certain values of volume flow rate and amplitude ratio but it decreases with increasing n at another certain values of volume flow rate and amplitude ratio. Moreover, the friction force at flow separation points declares reflux phenomena in contraction region. We discuss behaviour of the vertical velocity, the shearing extra stress, the pressure rise and the friction force at flow separation points for the physical parameters of interest.

Keywords: Peristalsis, power-law fluid, trapping

I. Introduction

When a progressive wave-resulting from area contraction and relaxation of an extensible tube propagates along the length of the tube, a fluid contained in the tube is mixed and transported in the direction of the wave propagation as if it were squeezed out by the moving wall. This phenomenon, called Peristalsis, is an inherent property

of any tubular organ of the human body such as the ureter, the gastro-intestinal tract, or the small blood vessels.

The mechanics of peristalsis has been examined by a number of investigators. Latham [15] was probably the first to investigate the mechanism of peristalsis in relation to mechanical pumping. Lew et al [9] observed that Reynolds number in the small intestine was very small. Shukla et al. [10] have investigated the effects of peripheral-layer viscosity on peristaltic transport of a bio-fluid in uniform tube and have used the long wavelength approximation as in Shapiro et al [3]. Shapiro et al [3] investigated the fluid mechanics of peristaltic pumping in connection with the function of systems such as the ureter, the gastro-intestinal tract, the small blood vessels, and other glandular ducts. They found that there was two physiologically significant phenomena called reflux and trapping in peristaltic flow. Yin and Fung [8] have investigated peristaltic waves in circular cylindrical tubes using a perturbation method. Srivastava and Srivastava [11] have investigated the effects of power law fluid in uniform and non-uniform tube under zero Reynolds number and long wavelength approximations. Pozrikidis [6] has investigated a study of peristaltic flow under the assumption of creeping motion and used the boundary integral method for Stokes flow. Takabatake and Ayukawa [13] presented finite-difference solutions for two-dimensional peristaltic flows. The influences of the magnitudes of wave amplitude, wavelength and Reynolds number on the flow are investigated through numerical calculations, and the results are compared with those of the perturbation analysis. Takabatake et al [14] solved the problem of peristaltic pumping in an axisymmetric tube by generalizing the numerical method of Takabatake and Ayukawa [13] to the axisymmetric case. Also, they have studied the trapping and reflux phenomena at the centerline. El Shehawey and Mekheimer [7] have investigated the effects of couple-stresses in peristaltic transport of fluid and have used a perturbation method as in Fung and Yih [16]. Siddiqui and Schwarz [4] have investigated peristaltic flow of a second-order fluid in tube and studied the flow separation at the centerline (centerline trapping). Abd El Hakeem and El Misery [2] have investigated peristaltic pumping of Carreau fluid in presence of an endoscope. Abd El Hakeem Abd El Naby et al [1] studied the flow separation on the wall. Also, they found that the trapping region at the wall decreases with increasing volume flow rate

In this paper, we investigated the reflux and trapping phenomena at the wall in non-Newtonian power-law fluid through uniform tube in the small intestine.

II. Formulation and analysis:

We consider the peristaltic flow of an incompressible non-Newtonian power-law fluid through a tube of average radius a. The geometry of the wall surface is described as figure (1):

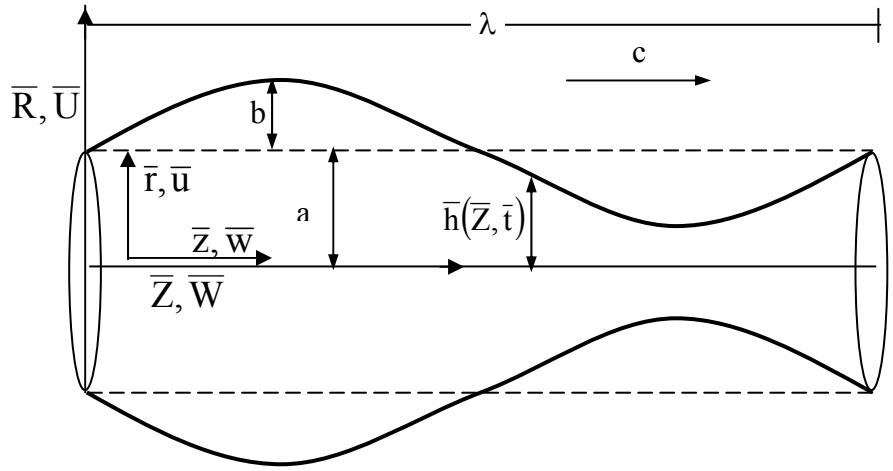

Figure (1): The flow separation through peristaltic motion in an uniform tube.

$$\bar{h}(\bar{Z}, \bar{t}) = a + b\,\mathrm{Sin}\left(\frac{2\pi}{\lambda}(\bar{Z} - c\bar{t})\right), \tag{2.1}$$

where b is the wave amplitude, λ is the wavelength, $\bar{t}$ is the time and c is the wave speed. We will assume that there is no motion of the wall in the axial direction.

We choose the cylindrical coordinate system $(\bar{R}, \bar{Z})$, where the $\bar{Z}$-axis lies along the center–line of the tube, and $\bar{R}$ is the distance measured radially. In the fixed coordinates $(\bar{R}, \bar{Z})$, the flow in the tube is unsteady but if we choose moving coordinates $(\bar{r}, \bar{z})$, which travel in the $\bar{Z}$ - direction with the same speed as the wave, then the flow can be treated as steady. The coordinates frame are related through:

$$\bar{z} = \bar{Z} - c\bar{t}, \quad \bar{r} = \bar{R}, \tag{2.2}$$

$$\bar{w} = \bar{W} - c, \quad \bar{u} = \bar{U}, \tag{2.3}$$

where $\bar{U}, \bar{W}$ and $\bar{u}, \bar{w}$ are the velocity components in the radial and axial directions in the fixed and moving coordinates respectively.

Equations of motion and boundary conditions in the moving coordinates are

Continuity equation:

$$\frac{1}{\bar{r}}\frac{\partial(\bar{r}\,\bar{u})}{\partial\,\bar{r}} + \frac{\partial\,\bar{w}}{\partial\,\bar{z}} = 0. \tag{2.4}$$

Navier-Stokes equations:

$$\rho\left(\bar{u}\frac{\partial\,\bar{u}}{\partial\,\bar{r}} + \bar{w}\frac{\partial\,\bar{u}}{\partial\,\bar{z}}\right) = -\frac{\partial\bar{P}}{\partial\,\bar{r}} - \left(\frac{1}{\bar{r}}\frac{\partial(\bar{r}\,\bar{\tau}_{11})}{\partial\,\bar{r}} + \frac{\partial\,\bar{\tau}_{31}}{\partial\,\bar{z}} - \frac{\bar{\tau}_{22}}{\bar{r}}\right), \tag{2.5}$$

$$\rho\left(\bar{u}\frac{\partial\,\bar{w}}{\partial\,\bar{r}} + \bar{w}\frac{\partial\,\bar{w}}{\partial\,\bar{z}}\right) = -\frac{\partial\,\bar{P}}{\partial\,\bar{z}} - \left(\frac{1}{\bar{r}}\frac{\partial(\bar{r}\,\bar{\tau}_{13})}{\partial\,\bar{r}} + \frac{\partial\,\bar{\tau}_{33}}{\partial\,\bar{z}}\right). \tag{2.6}$$

Constitutive equation:

$$\eta = m\,\bar{\dot{\gamma}}^{(n-1)}, \tag{2.7}$$

$$\bar{\tau}_{ij} = -m\,\bar{\dot{\gamma}}^{(n-1)}\bar{\dot{\gamma}}_{ij}, \tag{2.8}$$

where ρ is the density, τ_{ij}, i, j = 1,2,3 are the components of the extra stress tensor, $\bar{P}$ is the pressure, m is the consistency, n is the dimensionless power law index (when n=1, then m=μ is the Newtonian viscosity of the fluid) and $\bar{\dot{\gamma}}$ is defined as :

$$\bar{\dot{\gamma}} = \sqrt{\frac{1}{2}\sum_i\sum_j \bar{\dot{\gamma}}_{ij}\bar{\dot{\gamma}}_{ij}}\ . \tag{2.9}$$

The rate of strain tensor $\bar{\dot{\gamma}}_{ij}$ has the components

$$\bar{\dot{\gamma}}_{11} = 2\frac{\partial \bar{u}}{\partial \bar{r}},\ \bar{\dot{\gamma}}_{22} = \frac{2\bar{u}}{\bar{r}},\ \bar{\dot{\gamma}}_{33} = 2\frac{\partial \bar{w}}{\partial \bar{z}} \text{ and } \bar{\dot{\gamma}}_{13} = \bar{\dot{\gamma}}_{31} = \frac{\partial \bar{u}}{\partial \bar{z}} + \frac{\partial \bar{w}}{\partial \bar{r}}. \tag{2.10}$$

Boundary conditions:

$$\bar{u} = 0, \quad \frac{\partial \bar{w}}{\partial \bar{r}} = 0 \qquad \text{for} \quad \bar{r} = 0, \tag{2.11a}$$

$$\bar{w} = -c, \quad \bar{u} = -c\frac{d\bar{h}}{d\bar{z}} \quad \text{for} \quad \bar{r} = \bar{h}. \tag{2.11b}$$

Using the dimensionless variables appearing in equations (2.1-2.11) introducing Reynolds number (Re), wave number (δ) as follows:

$$r = \frac{\bar{r}}{a}, \quad R = \frac{\bar{R}}{a}, \quad z = \frac{\bar{z}}{\lambda}, \quad Z = \frac{\bar{Z}}{\lambda}, \quad u = \frac{\lambda\bar{u}}{ac},$$

$$U = \frac{\lambda\bar{U}}{ac}, \quad w = \frac{\bar{w}}{c}, \quad W = \frac{\bar{W}}{c}, \quad P = \frac{a^{n+1}\bar{P}}{mc^n\lambda}, \quad t = \frac{c\bar{t}}{\lambda},$$

$$\tau_{ij} = \frac{a^n\,\bar{\tau}_{ij}}{mc^n} \quad \dot{\gamma}_{ij} = \frac{a\,\bar{\dot{\gamma}}_{ij}}{c}, \quad \dot{\gamma} = \frac{a\,\bar{\dot{\gamma}}}{c}, \quad Re = \frac{\rho\, a^n}{mc^{n-2}}, \quad \delta = \frac{a}{\lambda},$$

$$\text{and} \quad h = \frac{\bar{h}}{a} = 1 + \phi\,\mathrm{Sin}(2\pi z), \tag{2.12}$$

where $\phi = \frac{b}{a} < 1$ is the amplitude ratio.

Continuity equation becomes:

$$\frac{1}{r}\frac{\partial(ru)}{\partial r} + \frac{\partial w}{\partial z} = 0. \tag{2.13}$$

Navier-Stokes equations become:

$$\mathrm{Re}\,\delta^3\left(u\frac{\partial u}{\partial r}+w\frac{\partial u}{\partial z}\right)=-\frac{\partial P}{\partial r}-\delta\frac{1}{r}\frac{\partial(r\tau_{11})}{\partial r}-\delta^2\frac{\partial\tau_{31}}{\partial z}+\delta\frac{\tau_{22}}{r}, \tag{2.14}$$

$$\mathrm{Re}\,\delta\left(u\frac{\partial w}{\partial r}+w\frac{\partial w}{\partial z}\right)=-\frac{\partial P}{\partial z}-\frac{1}{r}\frac{\partial(r\tau_{13})}{\partial r}-\delta\frac{\partial\tau_{33}}{\partial z}, \tag{2.15}$$

$$\tau_{ij}=-\dot{\gamma}^{(n-1)}\dot{\gamma}_{ij}, \tag{2.16}$$

with the dimensionless boundary conditions:

$$u=0,\ \frac{\partial w}{\partial r}=0 \quad \text{for } r=0, \tag{2.17a}$$

$$w=-1,\ u=-\frac{dh}{dz} \quad \text{for } r=h. \tag{2.17b}$$

The components of rate of strain tensor in the dimensionless form become

$$\dot{\gamma}_{11}=2\delta\frac{\partial u}{\partial r},\ \dot{\gamma}_{22}=\frac{2\delta u}{r},\ \dot{\gamma}_{33}=2\delta\frac{\partial w}{\partial z} \text{ and } \dot{\gamma}_{13}=\dot{\gamma}_{31}=\frac{\partial w}{\partial r}+\delta^2\frac{\partial u}{\partial z}. \tag{2.18}$$

Also, $\dot{\gamma}$ is defined in the dimensionless form as following:

$$\dot{\gamma}=\sqrt{\frac{1}{2}\delta^2\left(\dot{\gamma}_{11}^2+\dot{\gamma}_{22}^2+\dot{\gamma}_{33}^2\right)+\frac{1}{2}\left(\dot{\gamma}_{13}^2+\dot{\gamma}_{31}^2\right)}, \tag{2.19}$$

Using the long wavelength approximation and neglecting the wave number then from equations (2.16), (2.18) and (2.19) shearing extra stress becomes

$$\tau_{13}=\tau_{31}=\left(-\frac{\partial w}{\partial r}\right)^n. \tag{2.20}$$

Navier-Stokes equations reduce to:

$$\frac{\partial P}{\partial z}=-\frac{1}{r}\frac{\partial}{\partial r}\left(r\left(-\frac{\partial w}{\partial r}\right)^n\right), \tag{2.21}$$

$$\frac{\partial P}{\partial r}=0. \tag{2.22}$$

Integrating equation (2.21) with using equations (2.22) and (2.17), we get

$$w=c_0 r^{\left(\frac{n+1}{n}\right)}+c_1, \tag{2.23}$$

where

$$c_0=-\frac{n}{n+1}\left(-\frac{1}{2}\frac{dP}{dz}\right)^{\frac{1}{n}},\quad c_1=\frac{n}{n+1}\left(-\frac{1}{2}\frac{dP}{dz}\right)^{\frac{1}{n}}h^{\left(\frac{n+1}{n}\right)}-1.$$

From Siddiqui and Schwarz [4] and Abd El Hakeem Abd El Naby et al [1] the dimensionless time-mean flow rate Θ in moving coordinates is given by

$$\Theta = f + \frac{1}{2}\left(1 + \frac{\phi^2}{2}\right), \tag{2.24}$$

where

$$f = \int_0^h r\, w dr. \tag{2.25}$$

Integrating equation (2.25) , with using equation (2.23), we obtain

$$\frac{dP}{dz} = -2\left(\frac{3n+1}{n}\right)^n \frac{\left(2f + h^2\right)^n}{h^{3n+1}}. \tag{2.26}$$

The pressure rise ΔP_λ and the friction force F_λ (at the wall) in the tube of length λ, in their non-dimensional forms, are given by

$$\Delta P_\lambda = \int_0^l \left(\frac{dP}{dz}\right) dz\,, \tag{2.27}$$

$$F_\lambda = \int_0^l h^2 \left(-\frac{dP}{dz}\right) dz\,. \tag{2.28}$$

Substituting from equation (2.26) into equation (2.23), we get:

$$w = c_0 r^{\left(\frac{n+1}{n}\right)} + c_1, \tag{2.29}$$

where

$$c_0 = -\left(\frac{3n+1}{n+1}\right)\frac{\left(2f + h^2\right)}{h^{\left(\frac{3n+1}{n}\right)}}, \quad c_1 = \left(\frac{3n+1}{n+1}\right)\frac{2f}{h^2} + \left(\frac{2n}{n+1}\right).$$

Integrating equation (2.13) and using equation (2.29), we get:

$$u = -\frac{n}{3n+1} c_0' r^{\frac{2n+1}{n}} - \frac{c_1'}{2} r, \tag{2.30}$$

where the dash means differentiation with respect to z .
From equations (2.20) and (2.29) shearing extra stress is given by:

$$\tau_{13} = \left(\left(\frac{3n+1}{n}\right)\frac{\left(2f + h^2\right)}{h^3}\right)^n. \tag{2.31}$$

A condition frequently used to predict separation in boundary layer theory is to set the vorticity equal to zero on the boundary, setting

$$\xi = \frac{\partial u}{\partial z} - \frac{\partial w}{\partial r} = 0 \quad \text{for } r = h\,. \tag{2.32}$$

Substituting from equations (2.29) and (2.30) into equation (2.32), we get:

$$\frac{2(3n+1)}{n} f\left(1+h'^{2}\right)+h^{2}\left(\frac{(2n+1)}{n}h'^{2}-h\,h''+\frac{(3n+1)}{n}\right)=0\,. \tag{2.33}$$

Substituting from equations (2.12) and (2.24) into equation (2.33) we get:

$$\frac{2(3n+1)}{n}\left(\Theta-\frac{1}{2}\left(1+\frac{\phi^{2}}{2}\right)\right)\left(1+\left(2\pi\phi\ \mathrm{Cos}2\pi z\right)^{2}\right)+\left(1+\phi\ \mathrm{Sin}2\pi z\right)^{2}\times$$
$$\left(\frac{(2n+1)}{n}\left(2\pi\phi\ \mathrm{Cos}2\pi z\right)^{2}-\left(1+\phi\ \mathrm{Sin}2\pi z\right)\left(-4\pi^{2}\phi\ \mathrm{Sin}2\pi z\right)+\frac{(3n+1)}{n}\right)=0. \tag{2.34}$$

Solving equation (2.34) numerically to get flow separation points z_s. Hence, we substitute the flow separation points z_s into equations (2.26-2.28) and equation (2.31), we get:

$$\frac{dP}{dz}=-2\left(\frac{3n+1}{n}\right)^{n}\frac{\left(2f+h_s^{2}\right)^{n}}{h_s^{3n+1}}, \tag{2.35}$$

$$\left(\Delta P_{\lambda}\right)_s=\int_0^1\left(\frac{dP}{dz}\right)_s dz\ , \tag{2.36}$$

$$\left(F_{\lambda}\right)_s=\int_0^1 h_s^{2}\left(-\frac{dP}{dz}\right)_s dz_s, \tag{2.37}$$

$$\left(\tau_{13}\right)_s=\left(\left(\frac{3n+1}{n}\right)\frac{\left(2f+h_s^{2}\right)}{h_s^{3}}\right)^{n}. \tag{2.38}$$

where

$$h_s=1+\phi\,\mathrm{Sin}\,2\pi z_s\,. \tag{2.39}$$

From equation (2.30), the vertical velocity component at separation points on the wall is given by :

$$u_s=-h_s'=-2\pi\phi\ \mathrm{Cos}\,2\pi z_s. \tag{2.40}$$

III. Numerical results and discussion

We discuss the phenomenon of flow separation (trapping) through the figures (2-3) where the separated flow phenomenon means that a bolus (defined as a volume of fluid bounded by closed streamlines in the wave frame) is transported at the wave speed.

The flow separation position has longitudinal component z_s and vertical component h_s on the wall surface. Figure (2) shows that the relation between h_s, which given by equation (2.39), and ϕ. We notice that, at {{ϕ <0.5, Θ=0.4} and {ϕ <0.7, Θ=0.6} for different values of n} h_s decreases with increasing ϕ, but at {Θ=0.2, {0.5 ≤ ϕ, Θ=0.4} and {0.7 ≤ ϕ, Θ=0.6} for different values of n} h_s increases with increasing ϕ. Furthermore, h_s decreases with increasing Θ, but it

increases with increasing power law index n. Also, the relation is non linear for different values of volume flow rate Θ and n.

Figure (3) shows that the relation between z_s, which given by equation (2.34), and ϕ. We notice that, at {{ϕ <0.6, Θ=0.2}, Θ=0.4 and Θ=0.6, for different values of n} there exist two values of z_s one of them approaches to inlet of contraction region and the other approaches to outlet of contraction region. The regoin of flow separation for z_s increases with increasing Θ and with decreasing n in the forward of contraction region but it decreases with increasing Θ and with decreasing n in the backward of contraction region. Moreover, at {{$0.6 \le \phi$, Θ=0.2} for different values of n} there exist two values of z_s one of them into inlet of relaxation region and the other into outlet of relaxation region. Furthermore, the region of flow separation for z_s is independent approximately of ϕ at inlet and outlet of relaxation region. Figures (2-3) show that non-separation points of the flow occur at {ϕ <0.04, Θ=0.2, for different values of n}, {{ϕ <0.08, n=1}, {ϕ <0.1, n=$\frac{1}{2}$}, {ϕ <0.13, n=$\frac{1}{3}$}, Θ=0.4} and {{ϕ <0.15, n=1}, {ϕ <0.2, n=$\frac{1}{2}$}, {ϕ <0.27, n=$\frac{1}{3}$}, Θ=0.4}.

Figure (4) shows that the relation between the radial velocity u_s of the fluid, which given by equation (2.40), and ϕ. We notice that, the magnitude of u_s increases with increasing ϕ and n in contraction region but it decreases with increasing Θ in contraction region. Also, at $\{0.6 \le \phi \le 1, \Theta=0.2\}$ for different values of n in relaxation region, the magnitude of u_s increases with increasing ϕ and it is independent approximately of n. Furthermore, the positive and negative values of u_s show that there exist a portion of fluid towards to forward of contraction region and the other towards to backward of contraction region. Figures (5-6) show that the relation between shearing extra stress $(\tau_{13})_s$ at flow separation points, which given by equation (2.38), and ϕ. We notice that, $(\tau_{13})_s$ increases with increasing n for Θ=0.6 and for $\{\Theta = 0.2,\ 0.04 \le \phi \le 0.42\}$ but it decreases with increasing n for $\{\Theta = 0.2,\ 0.42 < \phi \le 1\}$. Furthermore, $(\tau_{13})_s$ decreases with increasing amplitude ratio ϕ for Θ=0.2 and for $\{\Theta = 0.6,\ 0.63 \le \phi \le 1\}$ but it increases with increasing ϕ for $\{\Theta = 0.6,\ \phi < 0.63\}$. Figures (7-8) show that the relation between $(\tau_{13})_s$ and Θ. We notice that, $(\tau_{13})_s$ increases with increasing Θ. Moreover, $(\tau_{13})_s$ decreases with increasing n for $\{\phi = 0.2,\ 0 \le \Theta \le 0.18\}$ and $\{\phi = 0.8,\ 0 \le \Theta \le 0.3\}$, but it increases with increasing n for $\{\phi = 0.2,\ 0.18 < \Theta\}$ and $\{\phi = 0.8,\ 0.3 < \Theta\}$. Figure (9) shows that the relation between the pressure rise $(\Delta P_\lambda)_s$ at flow separation points, which given by equation (2.36), and Θ. We notice that, at $\{0 \le \Theta < 0.28,$ n=1} and $\{0 \le \Theta < 0.2,$ n=1/3} $(\Delta P_\lambda)_s$ is independent approximately of ϕ, and the magnitude of $(\Delta P_\lambda)_s$ decreases with increasing Θ, but at $\{0.28 \le \Theta,$ n=1} and $\{0.2 \le \Theta,$ n=1/3} the magnitude of $(\Delta P_\lambda)_s$ increases with increasing Θ. Also, this relation shows that the magnitude of $(\Delta P_\lambda)_s$ approximately has the same values at the two values of the longitudinal component z_s for different values of Θ except at $\{\{0.5 < \Theta,\ 0.2 < \phi\}$ for

different values of n}. Figure (10) shows that the relation between the friction force $(F_\lambda)_s$ at flow separation points, which given by equation (2.37), and Θ. We notice that, at $\{0 \le \Theta < 0.28,\ n=1\}$ and $\{0 \le \Theta < 0.15,\ n=1/3\}$ $(F_\lambda)_s$ decreases with increasing Θ, but at $\{0.28 \le \Theta,\ n=1\}$ and $\{0.15 \le \Theta, n=1/3\}$ $(F_\lambda)_s$ increases with increasing Θ. Also, at $\{0.28 \le \Theta < 0.5\}$ $(F_\lambda)_s$ decreases with increasing ϕ, but it increases with decreasing n. Moreover, this relation shows that $(F_\lambda)_s$ approximately has the same values at the two values of the longitudinal component z_s for different values of volume flow rate Θ except at $\{\{0.5<\Theta<0.6,\ \phi=0.6\}$ for different values of n}. Moreover, the friction force $(F_\lambda)_s$ declare reflux phenomenon in contraction region. Also, figures (9-10) show that the pressure rise at flow separation points has the opposite behavior of friction force for different values of ϕ and Θ.

Without considering flow separation points, the results have been obtained by Shapiro et al [3], Siddiqui and Schwarz [4], Rao and Usha [5] and Li and Brasseur [12] showed that the trapping occurs at the centerline in cylindrical coordinates. Furthermore, Takabatake et al [14], showed that the trapping region decreases with increasing stream function. Also, they showed that the reflux takes place near the axis for large Reynolds number and/or for large wave number, where it occurs near the wall for small Reynolds number and small wave number as pointed out by Shapiro et al [3]. Abd El Hakeem Abd El Naby et al [1] studied flow separation through peristaltic motion of a Carreau fluid in uniform tube at the wall. Our results showed that the trapping region decreases with increasing volume flow rate but it increases with increasing power-law index n. Also, the trapping and the reflux phenomena occur at the wall for zero Reynolds number and zero wave number. These results agree with Abd El Hakeem Abd El Naby et al [1] for Newtonian case.

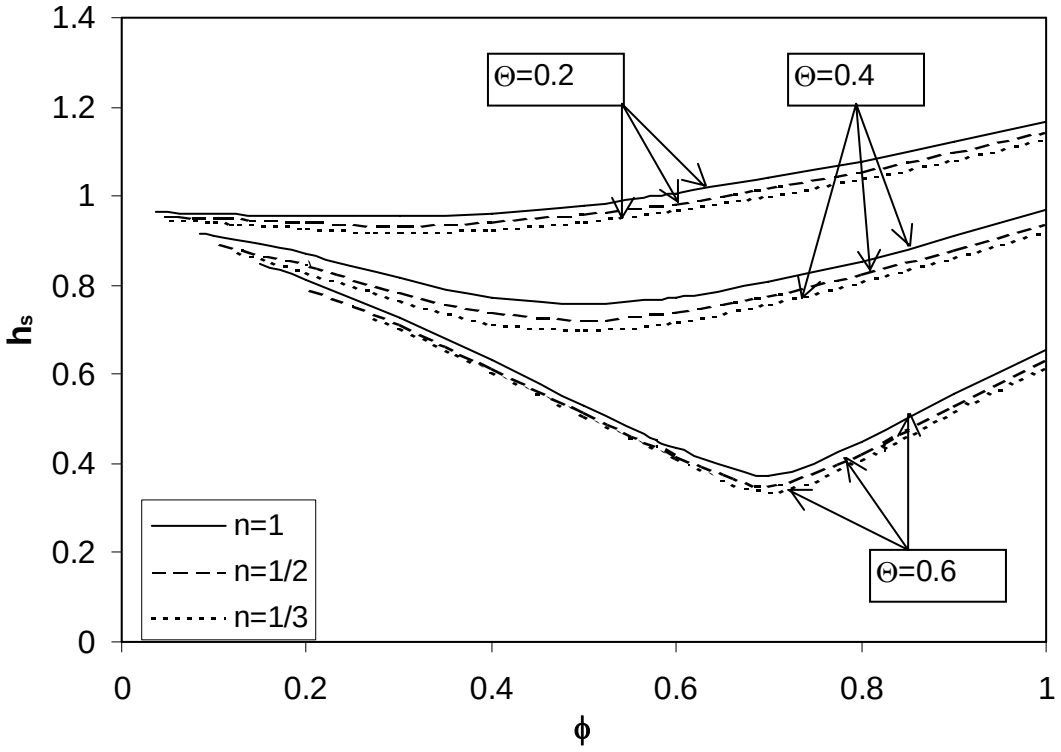

Figure (2): The vertical component on the wall surface at flow separation points versus amplitude ratio.

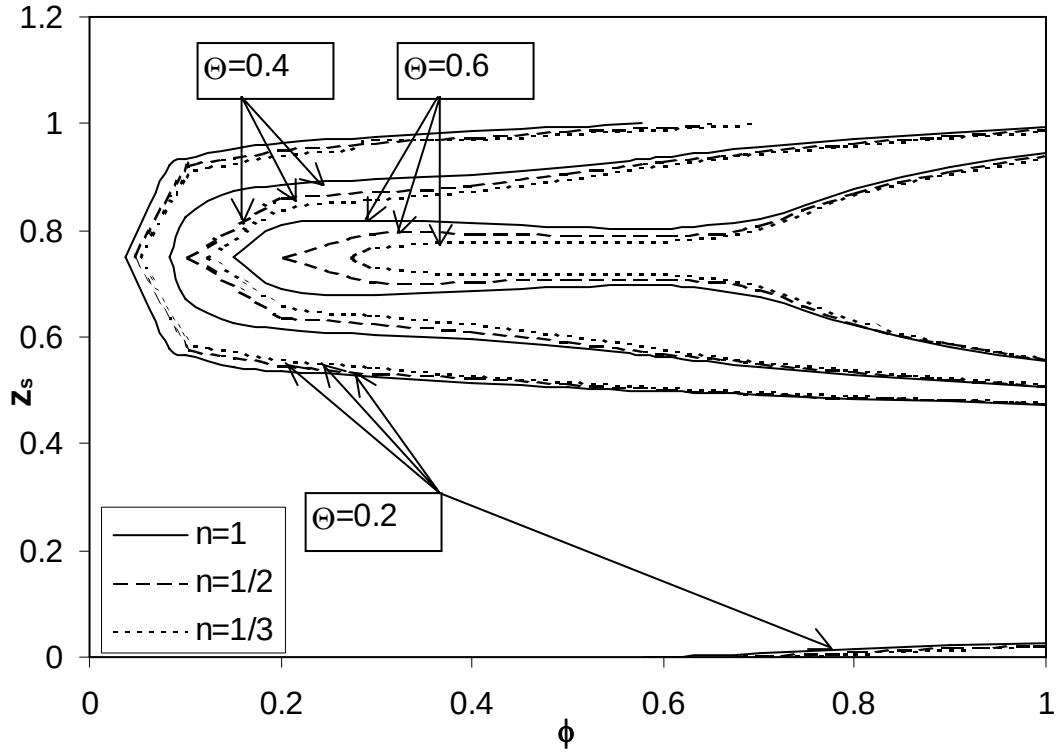

Figure (3): The longitudinal component of flow separation points versus amplitude ratio.

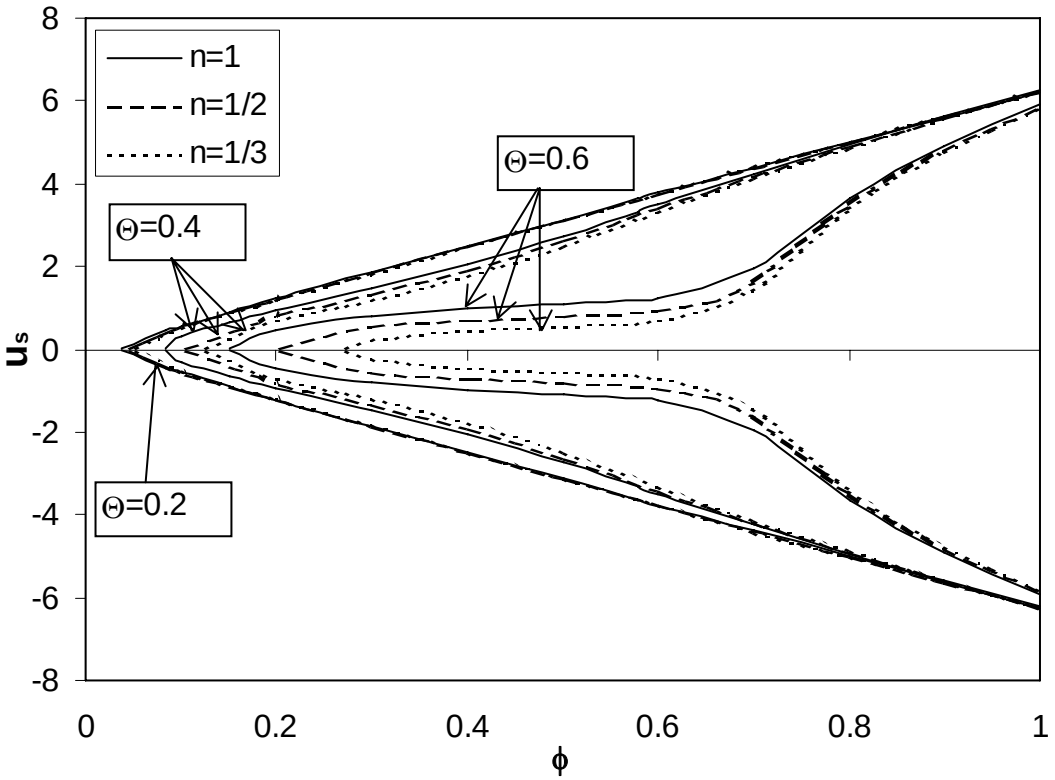

Figure (4): The radial velocity of the fluid at flow separation points versus amplitude ratio.

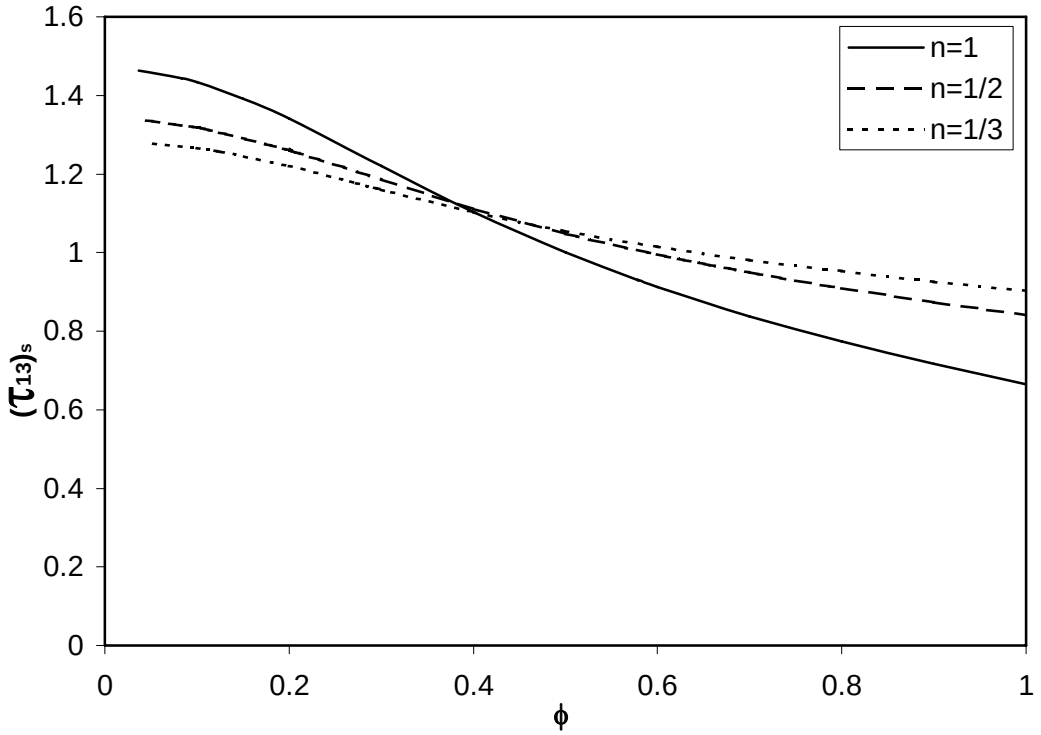

Figure (5): The shearing extra stress at flow separation points versus amplitude ratio for Θ=0.2.

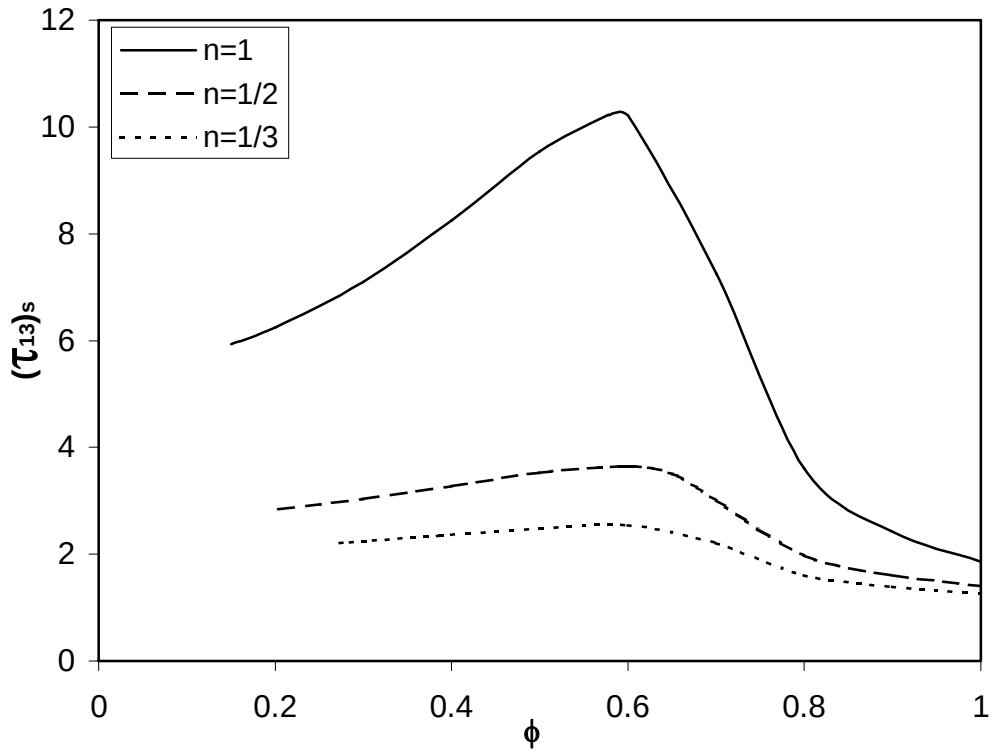

Figure (6): The shearing extra stress at flow separation points versus amplitude ratio for Θ=0.6.

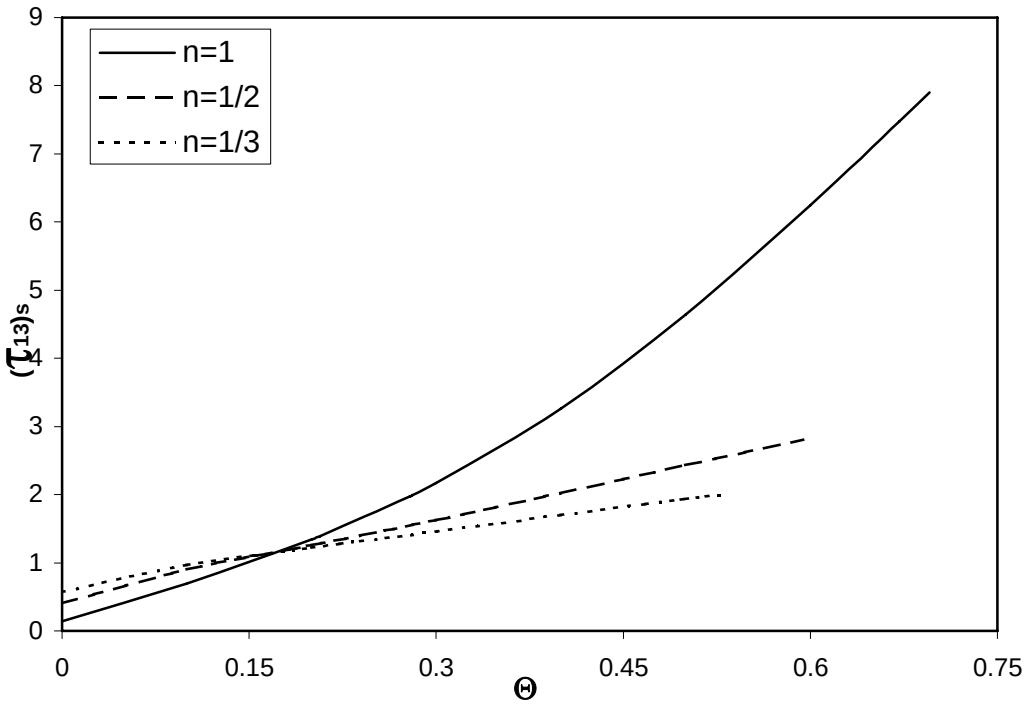

Figure (7): The shearing extra stress at flow separation points versus volume flow rate for ϕ =0.2.

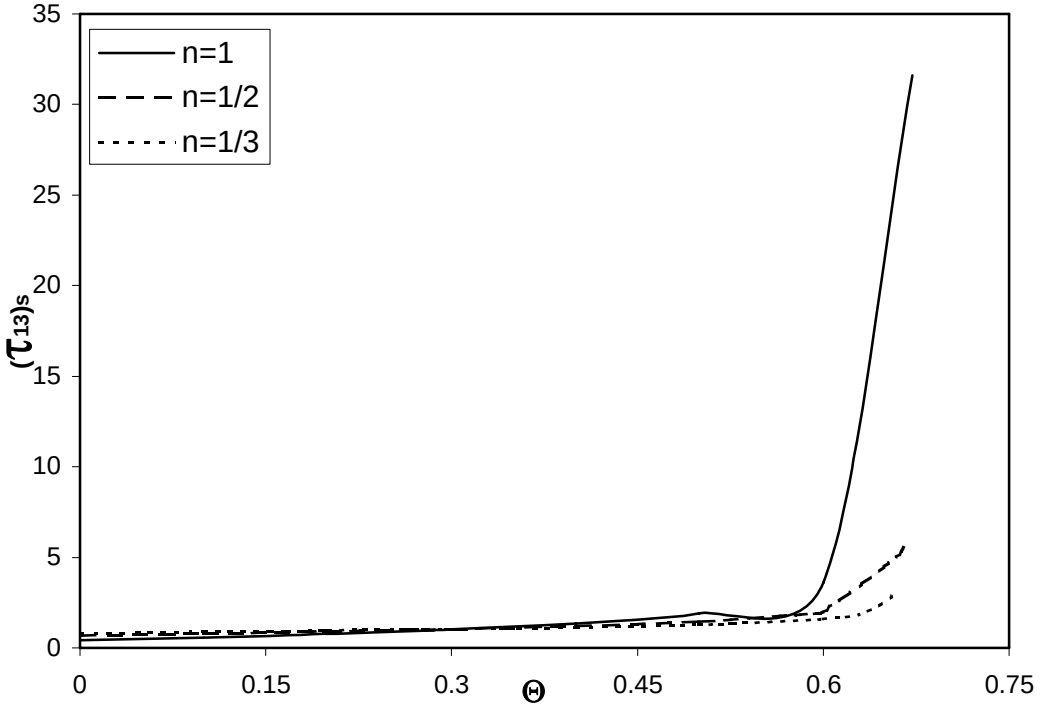

Figure (8): The shearing extra stress at flow separation points versus volume flow rate for ϕ =0.8.

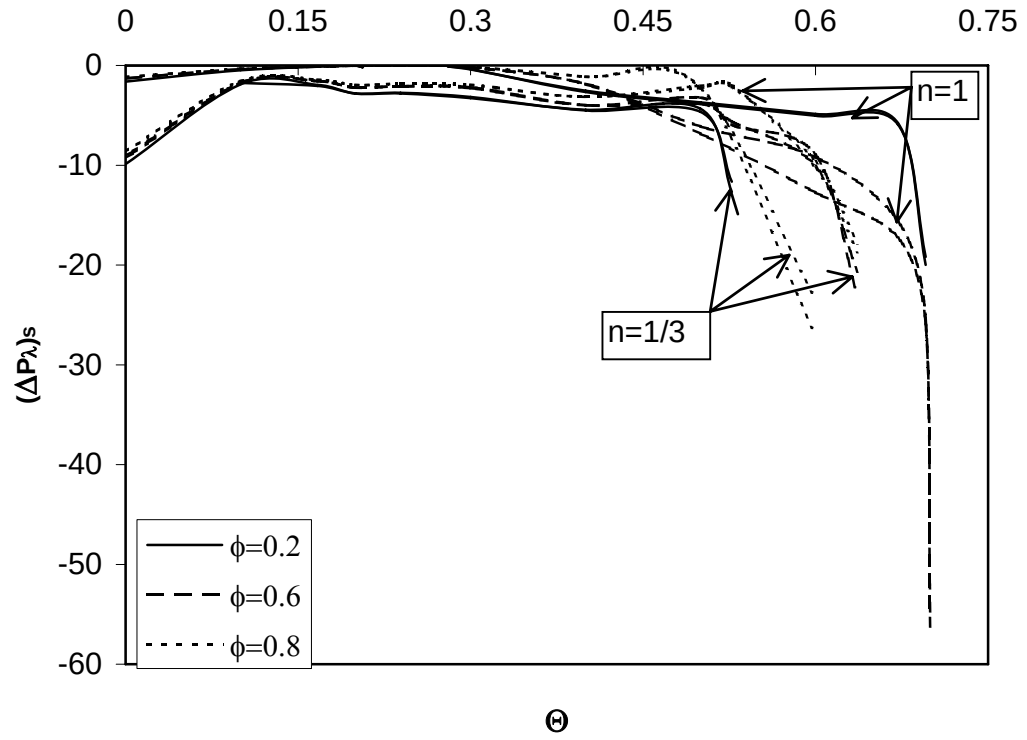

Figure (9): The pressure rise at flow separation points versus volume flow rate .

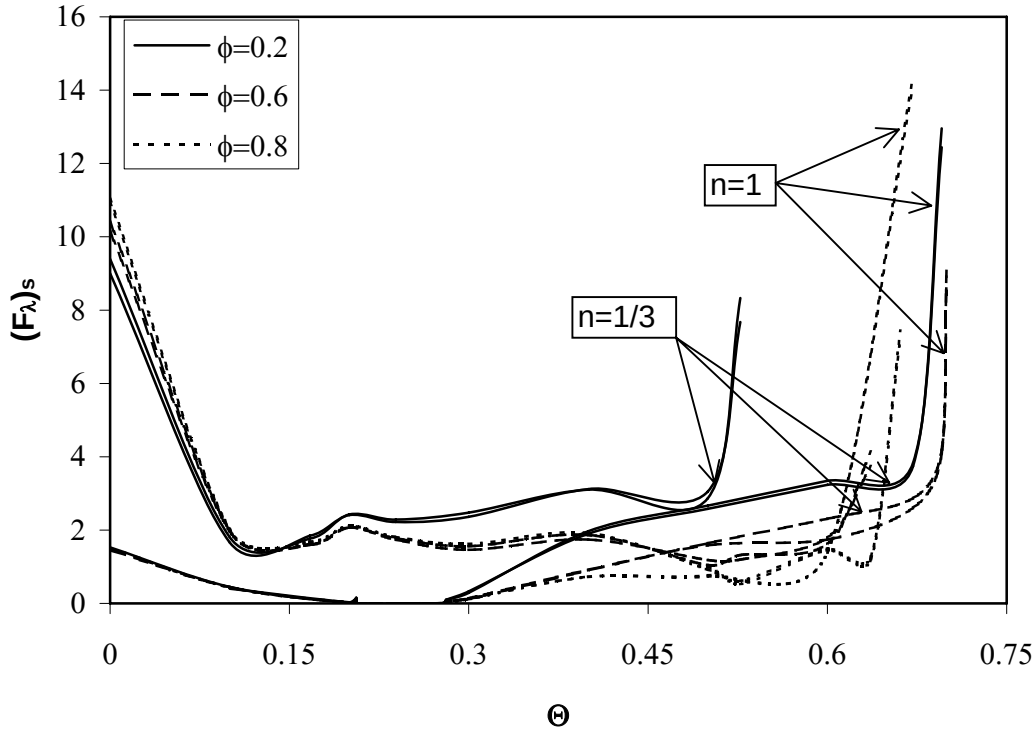

Figure (10): The friction force at flow separation points versus volume flow rate .

References:

[1] Abd El Hakeem Abd El Naby, A. E. M. El Misery and M. F. Abd El Kareem, Separation in the flow through peristaltic motion of a Carreau fluid in an uniform tube, Journal of Physica A: Statistical Mechanics and its Applications, 343C (2004), 1-14.

[2] A.M. Siddiqui and W.H. Schwarz, Peristaltic flow of a second-order fluid in tubes, J. non-Newtonian fluid Mech., 53 (1994), 257-284.

[3] A.H. Shapiro, M.Y. Jaffrin and S.L. Weinberg, Peristaltic pumping with long wavelengths at Reynolds number, J. Fluid Mech., 37 (1969), 799-825.

[4] A.M. Siddiqui and W.H. Schwarz, Peristaltic flow of a second-order fluid in tubes, J. non-Newtonian fluid Mech., 53 (1994), 257-284.

[5] A. R. Rao and S.J. Usha, Peristaltic transport of two immiscible viscous fluids in a circular tube, J.Fluid Mech., 298 (1995), 271-285.

[6] C. Pozrikidis, A study of peristaltic flow, J.Fluid Mech., 180 (1987), 515-527.

[7] E.F. ElShehawey and K.S. Mekheimer, Couple-stresses in peristaltic transport of fluids, J. Phys. D: Appl. Phys., 27 (1994), 1163-1170.

[8] F. Yin and Y.C. Fung, Peristaltic waves in circular cylindrical tubes, J. Applied Mechanics, 36 (1969), 579-587.

[9] H.S. Lew, Y.C. Fung and C. B. Lowenstein, Peristaltic carrying and mixing of chyme in the small intestine, J. Biomech., 4 (1971), 297-315.

[10] J.B. Shukla, R.S. Parihar, R.P. Rao and S.P. Gupta, Effects of peripheral layer viscosity on peristaltic pumping of a bio-fluid, J. Fluid Mech., 97 (1980), 225-237.

[11] L.M. Srivastava and V.P. Srivastava, Peristaltic transport of a non-Newtonian fluid: Applications to the vas deferens and small intestine, Annals of Biomedical Engineering, 13 (1985), 137-153.

[12] M. Li and J.G. Brasseur, Non-steady peristaltic transport in finitelength tubes, J. Fluid Mech., 248 (1993), 129–51.

[13] S. Takabatake and K. Ayukawa, Numerical analysis of two-dimensional peristaltic flows, J. Fluid Mech., 122 (1982), 439-465.

[14] S. Takabatake, K. Ayukawa and A. Mori, Peristaltic pumping in circular cylindrical tubes; a Numerical study of fluid transport and its efficiency, J. Fluid Mech., 193 (1988), 267-283.

[15] T.W. Latham, Fluid motion in a peristaltic pump, M.S. Thesis, MIT, Cambridge, MA, (1966).

[16] Y.C. Fung and C.S. Yih, Peristaltic transport, J. Appl. Mech., 35 (1968), 669-675.

Received: October 29, 2006